Monitoring potential ionospheric changes caused by Van earthquake (Mw 7.2)

Samed INYURT[1], Selcuk PEKER [2] and Cetin MEKIK[1]

[1]Zonguldak Bulent Ecevit University, Department of Geomatics Engineering, Zonguldak, Turkey (samed_inyurt@hotmail.com, cmekİk@hotmail.com)

[2] General Command of Mapping, Ankara, Turkey (selcuk-peker@hotmail.com)

ABSTRACT

Many scientists from different disciplines have studied earthquakes for many years. As a result of these studies, it has been proposed that some changes take place in the ionosphere layer before, during or after earthquakes, and the ionosphere should be monitored in earthquake prediction studies. This study investigates the changes in the ionosphere created by the earthquake with magnitude of Mw=7.2 in the northwest of the Lake Erçek which is located to the north of the province of Van in Turkey on 23 October 2011 and at 1.41 pm local time (-3 UT) with the epicenter of 38.75° N, 43.36° E using the TEC values obtained by the Global Ionosphere Models (GIM) created by IONOLAB-TEC and CODE. In order to see whether the ionospheric changes obtained by the study in question were caused by the earthquake or not, the ionospheric conditions were studied by utilizing indices providing information on solar and geomagnetic activities (F10.7 cm, Kp, Dst).

One of the results of the statistical test on the TEC values obtained from both models, positive and negative anomalies were obtained for the times before, on the day of and after the earthquake, and the reasons for these anomalies are discussed in detail in the last section of the study. As the ionospheric conditions in the analyzed days were highly variable, it was thought that the anomalies were caused by geomagnetic effects, solar activity and the earthquake.

Keywords: TEC, Van Earthquake, Ionosphere

1. INTRODUCTION

The ionosphere is the part of the atmosphere at the altitudes of 60 km to 1,100 km where there are ions and free electrons in considerable amounts that can reflect electromagnetic waves. It completely covers the thermosphere, one of the main layers of the atmosphere, but also includes some of the mesosphere and the exosphere.

Total Electron Content (TEC), which is defined as free electrons along a cylinder with a cross section of 1 m^2, is a suitable parameter to monitor the changes in the ionosphere. All signals that contain data that pass through or get reflected from the ionosphere, which is highly irregular and difficult to model, are affected by the structure of this layer.

Calculating Total Electron Content (TEC) is used directly to investigate the structure of the ionosphere. TEC is represented by the unit of TECU, and one TECU equals to $10^{16}\ el/m^2$ (Schaer, 1999). TEC is expressed in two ways: STEC (Slant Total Electron Content); the free electron content calculated along the slanted line between the receiver and the satellite, and VTEC (Vertical Total Electron Content); the free electron content calculated along the zenith of the receiver (Langley, 2002).

The ionosphere reacts to geomagnetic effect, solar activity, diurnal and seasonal effects, earthquake, and these factors cause irregularities in the ionosphere (Namgaladze et al, 2012, Li and Parrot, 2017).

Ionospheric changes have been studied in more than twenty countries today as precursors of earthquakes. Definition of ionospheric anomalies and feasibility studies of seismo-ionospheric precursors are still ongoing (Liu et al., 2010; He et al., 2012; Kamogawa and Kakinami**,** 2013; Heki and Enomoto, 2015; Pulinets and Davidenko, 2014; Masci et al., 2015; Yildirim et al., 2016; He and Heki, 2017; Kelley et al., 2017;Rozhnoi et al., 2015; Thomas et al., 2017; Ulukavak and Yalcinkaya 2017).

Our study aim is to investigate ionospheric changes possibly caused by Van earthquake while taking into account solar activity and magnetic storm affect. Van earthquake has very complex structure in terms of ionospheric conditions. When level of solar activity (F10.7cm) and magnetic storm (Kp and DsT) are considered, ionospheric conditions appear to be highly active before and after the earthquake. Therefore results obtained by statistical test should be interpreted carefully.

2. METHODOLOGY

2.1 IONOLAB-TEC Method:

The IONOLAB-TEC method developed by the department of Electrical and Electronics Engineering of Hacettepe University is a JAVA application that uses the Regularized TEC (D-TEI) algorithm (Arikan et al. 2004).

In this application, they developed a method that estimates VTEC values by using all GPS signals measured at a period of time in a day. While the measurements taken from the satellites with elevations of 60^o or higher are used, the measurements from the satellites with elevations of $10^o \ to \ 60^o$ are weighted by a Gauss function. The data from satellites with elevations lower than 10^o are not included in calculations to reduce multipath effects. In this method raw GPS data was used to determine VTEC value.

2.2 Global Ionosphere Model (GIM):

Global Ionospheric Maps are published in the IONEX (IONosphere map EXchange) format in a way that covers the entire world. The institutions that produce these maps in the world include CODE (Center for Orbit Determination in Europe, Switzerland), DLR (Fernerkundungstation Neustrelitz, Germany), ESOC (European Space Operations Centre, Germany), JPL (Jet Propulsion Laboratory, California), NOAA (National Oceanic and Atmospheric Administration, United States), NRCan (National Resources, Canada), ROB (Royal Observatory of Belgium, Belgium), UNB (University of New Brunswick, Canada), UPC (Polytechnic University of Catalonia, Spain), WUT (Warsaw University of Technology, Poland). In this study we used the GIM-TEC values produced by CODE in the IONEX format. In the dates they were analyzed, the temporal resolution of the TEC values was 2 hours, while their positional resolution was 2.5º by latitude and 5º by longitude. In order to calculate TEC values for a point whose latitude and longitude is known on the GIM-TEC maps created by CODE using more than 300 GNSS receivers around the world, the 4 TEC values that cover the point and the two-variable interpolation formula are given below.

$$E_{int}(\lambda_0 + p\Delta\boldsymbol{\lambda}, \beta_0 + q\Delta\beta) = (1-p)(1-q)E_{0.0} + p(1-q)E_{1.0} + q(1-p)E_{0.1} + pqE_{1.1} \quad (1)$$

p and q: $0 \leq p, q < 1$. (Schaer 1999)

$\Delta\lambda$ and $\Delta\beta$: Longitude and Latitude differences grid widths,

$\lambda_0 \ and \ \beta_0$: Initial longitude and latitude values,

$E_{0.0}, E_{1.0}, E_{0.1} \ ve \ E_{1.1}$: TEC values known in neighboring points,

E_{int}: TEC value to be found.

3. ANALYSIS TO DETERMINE EARTHQUAKE-RELATED TEC CHANGES

In order to investigate earthquake-related TEC changes, the TEC values for OZAL station (TUSAGA-Active CORS-TR) close to the epicenters GPS station was analyzed to determine

TEC value using the IONOLAB-TEC and GIM-TEC models. The correlation coefficient was obtained for the TEC values from both models between the dates 13.10.2011 and 02.11.2011 for the stations above. In addition to that, spatial analysis was applied to determine distribution characteristics of the ionospheric changes.

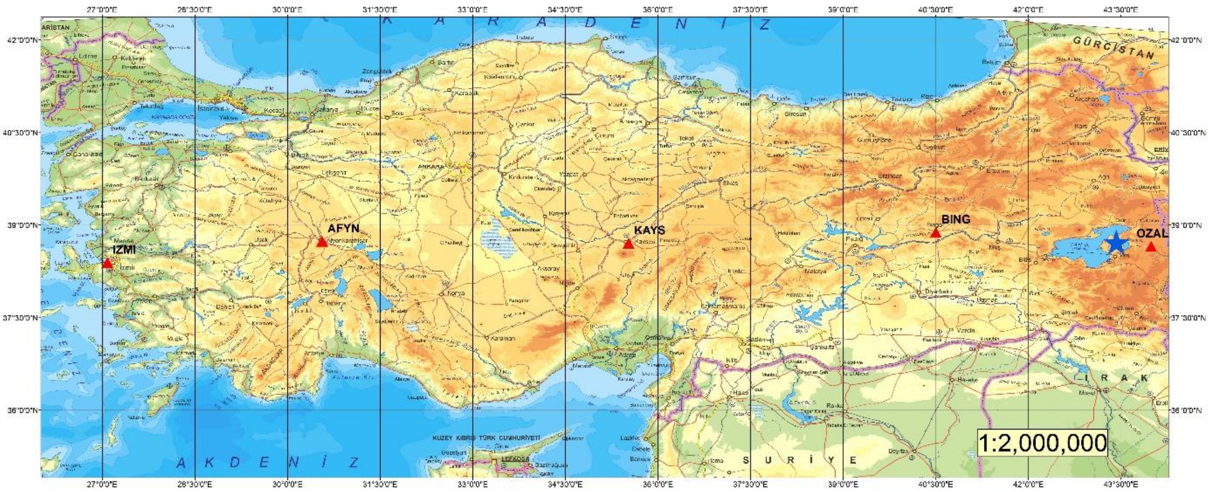

Figure 1. OZAL, IZMI, AFYN, KAYS AND BING Stations analyzed in the present work

Figure 1 shows the stations analyzed (represented by red triangles) and the epicenter of the earthquake represented by blue star. TEC values with the temporal resolution of two hours obtained from both the IONOLAB-TEC and GIM-TEC models for OZAL(37.06 N,36.15E) (station which is nearest station to epicenter of earthquake and the correlation coefficient was computed to explain linear relationship between two models. On the other hand, TEC values were also obtained using GIM model to explain spatial changes of ionosphere for IZMI(38.23N, 27.04E), AFYN(38.44N, 30.33E), KAYS(38.42N, 35.31E) and BING(38.53N, 40.30E) stations.

In order to determine the outlier values among the TEC values with a two-hour temporal resolution from both models, the TEC values obtained from both models between the dates 01.10.2011 and 10.10.2011, which were considered quiet in terms of geomagnetic and solar activity, were used to determine the upper boundary (UB) and the lower boundary (LB). By utilizing the TEC values from both models, the UB and LB values were calculated using the formulae $x+3\sigma$ and $x-3\sigma$. Here, x is the mean TEC value for the relevant epoch and σ is the standard deviation. If the TEC value in any epoch is higher than the upper boundary, it is a positive anomaly. Similarly if it is lower than the lower boundary, it is a negative anomaly. In order to investigate whether the anomalies before, on the day of and after the earthquake were caused by the earthquake or not, we also examined the (Kp*10), Dst and F10.7 cm indices, which provided information on the geomagnetic and solar activity for the days in which anomalies were detected.

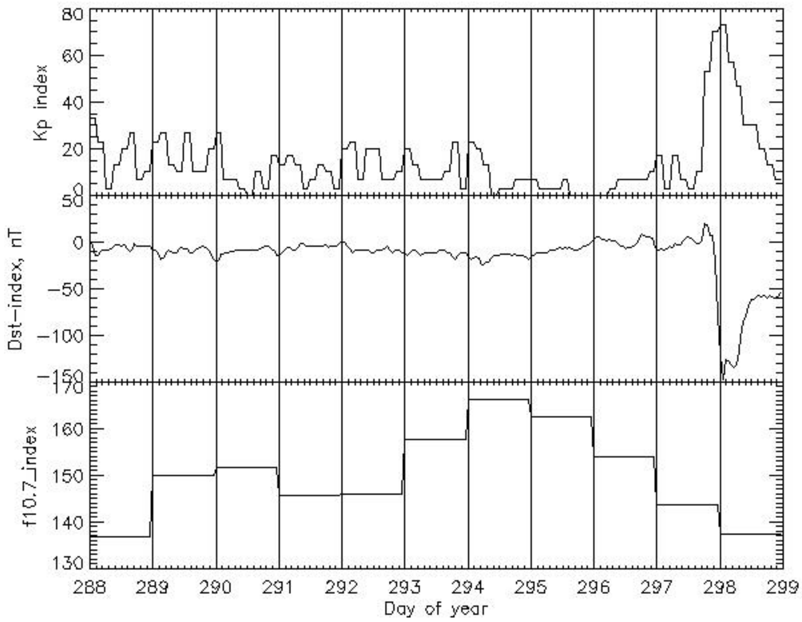

Figure 2. (Kp*10) DsT, F10.7 cm index variation from 288 to 299 in 2011 (URL-1)

Figures 2 shows that the (Kp*10), Dst and F10.7 cm indices that provide information on geomagnetic and solar activity 15.10.2011 to 25.10.2011.

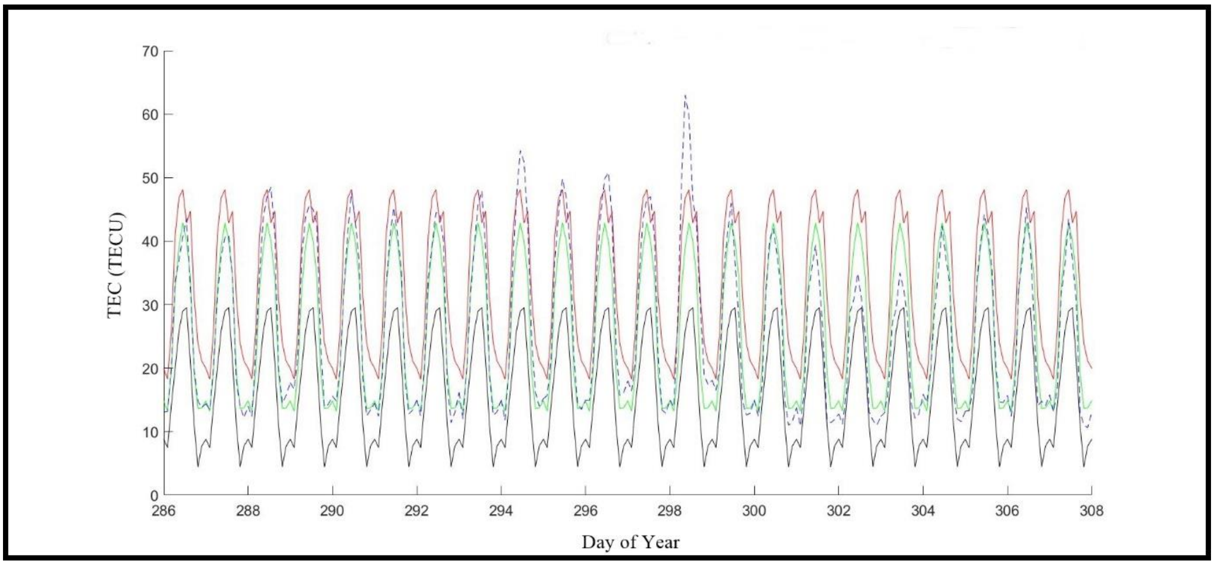

Figure 3. GIM-TEC Values for the OZAL Station. Black line shows lower bound TEC values, red line demonstrates upper bound TEC values, green line shows mean TEC values and dotted line indicates observed TEC values for every epoch.

GIM-TEC Anomaly Table for OZAL Station									
Number	**DOY**	**Hour**	**TEC Difference (TECU)**	**Type of Anomaly**	**Number**	**DOY**	**Hour**	**TEC Difference (TECU)**	**Type of Anomaly**
1	288	2	2.0	Positive	11	295	10	3.3	Positive
2	288	10	5.7	Positive	12	296	4	1.9	Positive
3	289	10	2.5	Positive	13	296	10	7.5	Positive
4	290	10	0.5	Positive	14	297	10	4.1	Positive
5	292	10	0.8	Positive	15	298	0	0.8	Positive
6	293	10	5.2	Positive	16	298	2	2.6	Positive
7	294	8	0.7	Positive	17	298	8	12.2	Positive
8	294	10	4.0	Positive	18	298	10	11.7	Positive
9	294	12	10.5	Positive	19	298	12	16.5	Positive
10	295	8	2.9	Positive	20	298	18	0.8	Positive

Table 1. OZAL Station Global Ionosphere Model Anomaly Table

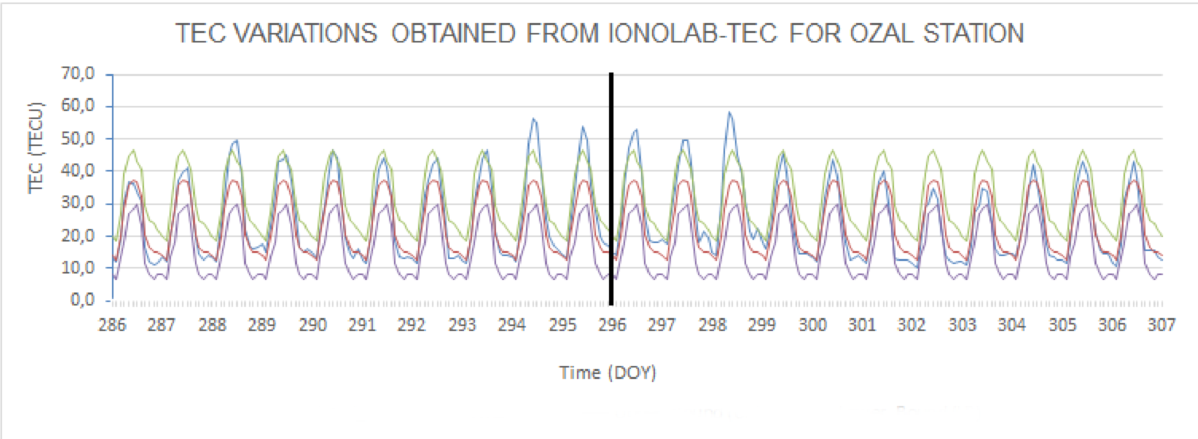

Figure 4 IONOLAB-TEC Values for the OZAL Station. Purple line shows lower bound TEC values, bottle green line demonstrates upper bound TEC values, red line shows mean TEC values and blue line indicates observed TEC values for every epoch.

IONOLAB-TEC Anomaly Table for OZAL Station									
Number	**DOY**	**Hour**	**TEC Difference (TECU)**	**Type of Anomaly**	**Number**	**DOY**	**Hour**	**TEC Difference (TECU)**	**Type of Anomaly**
1	288	10	5.1	Positive	9	297	10	6.0	Positive
2	289	10	1.6	Positive	10	298	0	2.2	Positive

3	290	10	0.9	Positive	11	298	2	2.4	Positive
4	292	12	0.6	Positive	12	298	4	4.1	Positive
5	293	10	3.5	Positive	13	298	6	3.0	Positive
6	294	12	11.8	Positive	14	298	8	7.3	Positive
7	295	10	7.4	Positive	15	298	10	13.6	Positive
8	296	10	9.6	Positive	16	298	12	12.8	Positive

Table 2. OZAL Station IONOLAB-TEC Anomaly Table

The correlation coefficient *r* between the TEC values calculated by both methods for the OZAL station was 0.98 demonstrating a strong positive relationship. The anomaly tables for this station are provided below (Tables 1 and 2).

In order to determine whether anomalies caused by earthquake or not, we also monitored spatial changes of TEC. In this regard, we investigated IZMI, AFYN, KAYS, BING stations TEC changes using GIM models. These receivers are located in same latitude as the OZAL station, thus we can obtain spatial TEC changes in Turkey for analyzed days.

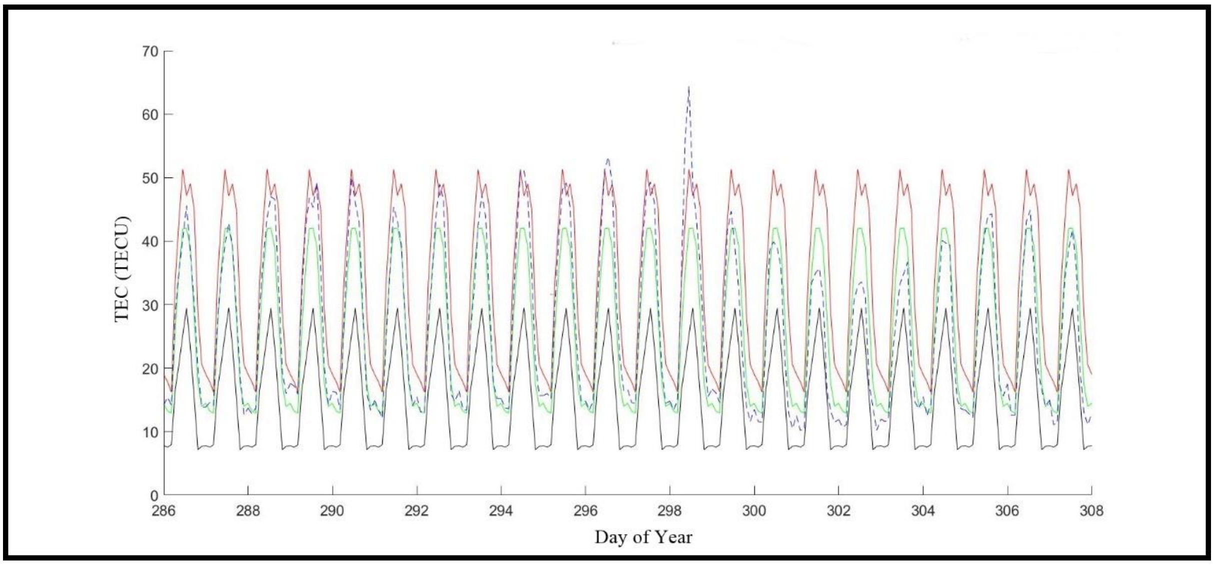

Figure 5 GIM-TEC Values for the IZMI Station. Black line shows lower bound TEC values, red line demonstrates upper bound TEC values, green line shows mean TEC values and dotted line indicates observed TEC values for every epoch.

GIM-TEC Anomaly Table for IZMI Station									
Number	**DOY**	**Hour**	**TEC Difference (TECU)**	**Type of Anomaly**	**Number**	**DOY**	**Hour**	**TEC Difference (TECU)**	**Type of Anomaly**
1	289	10	0.2	Positive	7	296	10	6.1	Positive
2	292	10	1.8	Positive	8	297	10	2.1	Positive
3	293	10	0.1	Positive	9	298	6	1.2	Positive
4	294	10	3.9	Positive	10	298	8	1.5	Positive

5	295	10	2.0	Positive	11	298	10	13.0	Positive
6	296	6	0.1	Positive	12	298	12	12.8	Positive

Table 3. IZMI Station GIM-TEC Anomaly Table

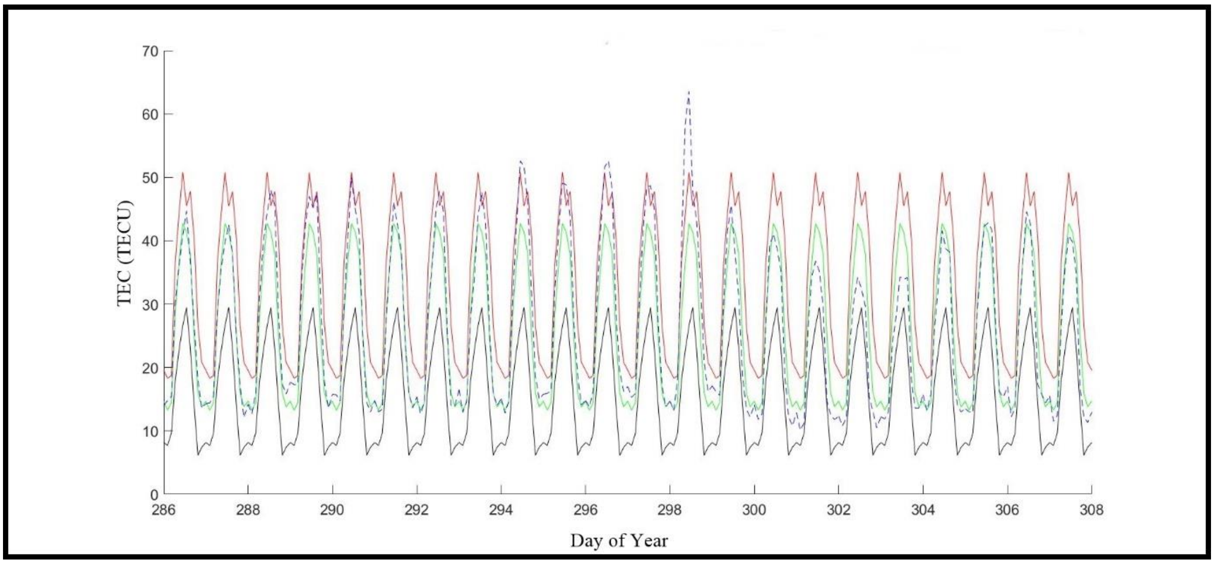

Figure 6 GIM-TEC Values for the AFYN Station. Black line shows lower bound TEC values, red line demonstrates upper bound TEC values, green line shows mean TEC values and dotted line indicates observed TEC values for every epoch.

GIM-TEC Anomaly Table for AFYN Station									
Number	**DOY**	**Hour**	**TEC Difference (TECU)**	**Type of Anomaly**	**Number**	**DOY**	**Hour**	**TEC Difference (TECU)**	**Type of Anomaly**
1	288	10	4.5	Positive	8	296	10	7.1	Positive
2	292	10	2.3	Positive	9	296	12	0.1	Positive
3	293	10	2.2	Positive	10	297	10	3.2	Positive
4	294	8	1.8	Positive	11	298	2	2.3	Positive
5	294	10	6.2	Positive	12	298	8	2.1	Positive
6	295	10	3.3	Positive	13	298	10	12.8	Positive
7	296	4	0.8	Positive	14	298	12	14.2	Positive

Table 4. AFYN Station GIM-TEC Anomaly Table

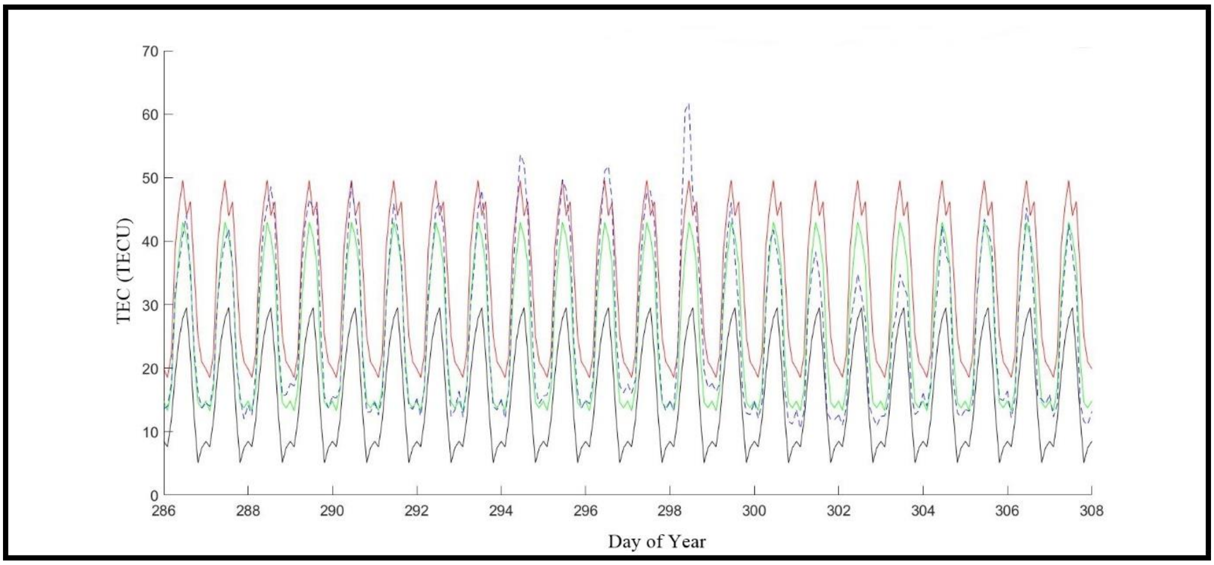

Figure 7 GIM-TEC Values for the KAYS Station. Black line shows lower bound TEC values, red line demonstrates upper bound TEC values, green line shows mean TEC values and dotted line indicates observed TEC values for every epoch.

GIM-TEC Anomaly Table for KAYS Station									
Number	**DOY**	**Hour**	**TEC Difference (TECU)**	**Type of Anomaly**	**Number**	**DOY**	**Hour**	**TEC Difference (TECU)**	**Type of Anomaly**
1	288	10	4.6	Positive	9	295	10	4.0	Positive
2	289	10	1.2	Positive	10	296	8	1.4	Positive
3	290	10	0.1	Positive	11	296	10	7.8	Positive
4	292	10	2.1	Positive	12	297	10	3.9	Positive
5	293	10	4.0	Positive	13	298	2	4.3	Positive
6	294	8	4.0	Positive	14	298	8	2.9	Positive
7	294	10	8.2	Positive	15	298	10	12.1	Positive
8	295	8	0.1	Positive	16	298	12	15.2	Positive

Table 5. KAYS Station GIM-TEC Anomaly Table

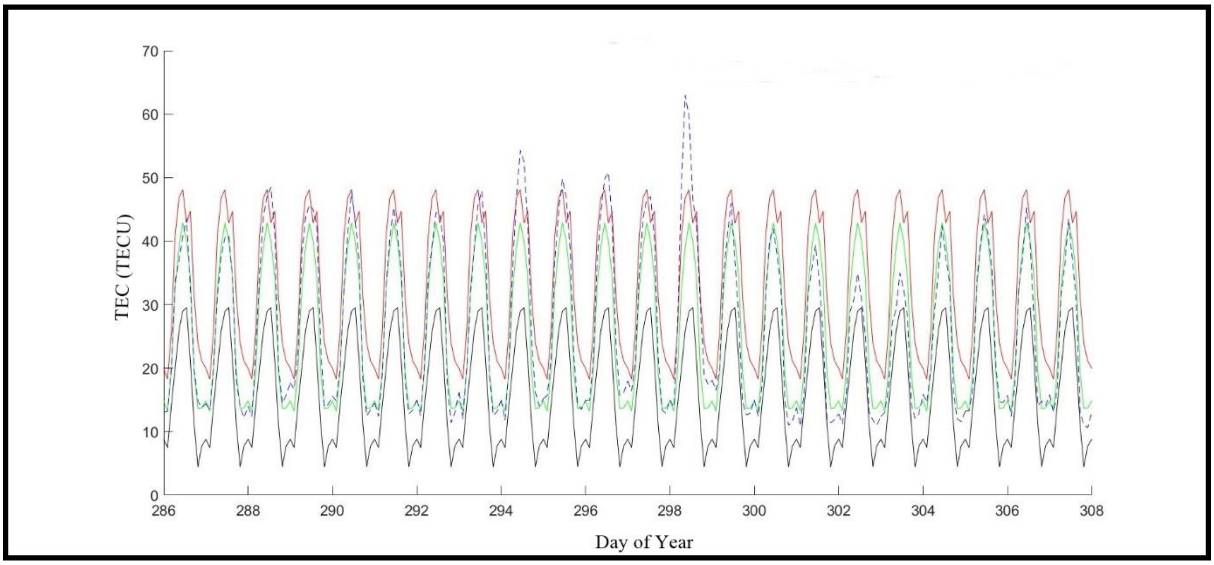

Figure 8 GIM-TEC Values for the BING Station. Black line shows lower bound TEC values, red line demonstrates upper bound TEC values, green line shows mean TEC values and dotted line indicates observed TEC values for every epoch.

GIM-TEC Anomaly Table for BING Station									
Number	DOY	Hour	TEC Difference (TECU)	Type of Anomaly	Number	DOY	Hour	TEC Difference (TECU)	Type of Anomaly
1	288	10	5.6	Positive	9	295	10	4.0	Positive
2	289	10	2.1	Positive	10	296	8	1.7	Positive
3	290	10	0.4	Positive	11	296	10	7.9	Positive
4	292	10	1.4	Positive	12	297	10	4.1	Positive
5	293	10	5.0	Positive	13	298	2	7.8	Positive
6	294	8	6.2	Positive	14	298	8	3.7	Positive
7	294	10	9.6	Positive	15	298	10	11.5	Positive
8	295	8	1.6	Positive	16	298	12	16.1	Positive

Table 6. BING Station GIM-TEC Anomaly Table

Tables (1-6) also depict the day and hour in which anomalies were observed, and the amount and type of the anomaly. The numbers of anomalies obtained in both models were very close to each other. The F10.7 cm index values between the days 288 and 292 were 136.9 sfu, 150 sfu, 151.6 sfu, 145.7 sfu, 146.1 sfu. Nwanko and Chakrabarti (2013) states that while F10.7 cm>151sfu is strong solar activity, 100 sfu<F10.7cm<150 sfu indicates moderate solar activity. The index values show that there was usually moderate solar activity. Therefore, the anomalies in question may be related to the earthquake or solar activity. The index values for the days

293, 294, 295 and 296 (the day of the earthquake) were 157.8 sfu, 166.3 sfu, 162.5 sfu and 153.9 sfu respectively. These values indicate strong solar activity. On the other hand, the ionosphere layer was quiet in these days in terms of geomagnetic conditions. The numbers of anomalies were higher than during the days 288-292 due to solar activity was stronger during these last days. Since solar activity was moderate in the day 297, the number of anomalies dropped. The solar activity on the day 298 was moderate, but there was strong geomagnetic activity (Dst -147 nt, Kp*10=73). The reason for the high numbers of anomalies on day 298 in both models is believed to be due to geomagnetic activity. This magnetic storm has caused different amount of TEC variation for all stations.

As another indicator, we extract ***Σ***ATEC (Totally TEC difference) to determine total amount of anomaly day by day for each analyzed days. ***Σ***ATEC shows total amount of anomaly for an analyzed day. For example 4.5 TECU is the sum of total TEC difference for the 24 hours of 288 in 2011 for AFYN station.

Stations/Anomaly Day	288 (***Σ***ATEC)	289 (***Σ***ATEC)	290 (***Σ***ATEC)	292 (***Σ***ATEC)	293 (***Σ***ATEC)	294 (***Σ***ATEC)	295 (***Σ***ATEC)	296 (***Σ***ATEC)	297 (***Σ***ATEC)	298 (***Σ***ATEC)
IZMI-GIM	-	0.2	-	1.8	0.1	3.9	2	6.2	2.1	28.5
AFYN-GIM	4.5	-	-	2.3	2.2	8	3.3	8	3.2	31.4
KAYS-GIM	4.6	1.2	0.1	2.1	4	12.2	4.1	9.2	3.9	34.5
BING-GIM	5.6	2.1	0.4	1.4	5	15.8	5.6	9.6	4.1	39.1
OZAL-GIM	7.7	2.5	0.5	0.8	5.2	15.2	6.2	9.4	4.1	44.5

Table 7. Total amount of anomaly in TECU for analyzed days

Table 7 shows total anomaly summary results obtained from analysis results. Positive anomalies were observed before and after the earthquake and amount of anomaly is nearly equal to each other in this earthquake. In addition to that, ***Σ***ATEC differences between stations are also similar to each other for in each analyzed day. Therefore this similarity causes from spatial variation of ionosphere.

Considering the analyzed days in general for all stations, it may be seen that it is difficult to identify earthquake-related anomalies as the solar activity and geomagnetic conditions before and after the earthquake were not quiet. Therefore, it is believed that the anomalies detected in the stations on days 293-296 may be related to the earthquake and/or solar activity, and the anomalies on days 297 and 298 may be related to the earthquake, solar activity and/or geomagnetic activity.

DISCUSSION AND CONCLUSION

Seismic ionospheric evalutions of Van earthquake have also been studied by many researchers (Arikan et al., (2012); Zolotov et al., 2012; Rolland 2013; Şentürk et al., 2018). Arikan et al., (2012) and Zolotov et al. (2012) determined some anomalies before and after the earthquake, but solar and magnetic conditions were not taken into account. On the other hand Şentürk et al. (2018) also obtained abnormal days before and after the earthquake and they evaluated solar activity and magnetic storm conditions for these abnormal days to explain possible causes of anomalies in detail. Some previous studies have also studied on both space weather and earthquake effect in the ionosphere (Yao et al., 2012; Le et al., 2013). They especially state that TEC enhancement may be related to geomagnetic storm and earthquake.

Şentürk et al. (2018) study also shows that there is no obvious anomaly caused only by earthquake.Therefore they suggest that a multidisciplinary study would be useful to identify ionospheric changes as an earthquake precursor under the disturbed space-weather conditions. This approach shows that their results agree with our study. Apart from our method, He et al. (2012) study states that detection of earthquake anomaly can be removed from measurement using (Multiresolution wavelet transfrom (MWT) method remove other effect like solar radiation. However this technique's main problem is that F10.7 cm is one value, TEC is 2 hours temporal resolution for one day. Thus we think that different temporal resolutions of F10.7 cm and TEC cause big obstacle to distinguish F10.7 effect on TEC value directly.

In the scope of this study, the TEC values for the stations IZMI, AFYN, KAYS, BING were obtained using the GIM-TEC and TEC values were also obtained using GIM-TEC and IONOLAB-TEC methods for OZAL station. In the comparison of the obtained values, it was seen that there was high correlation between the TEC values obtained by the two models for OZAL station. In order to detect earthquake-related TEC changes better, the TEC values created from both models for the period of 13.10.2011-02.11.2011 were used as reference to determine the upper bound and lower bound values. As a result of the statistical test, anomalies were found in all analyzed stations for before, on the day of and after the earthquake. In order to understand whether the anomalies obtained in both models were earthquake-related, the ionospheric conditions, geomagnetic activity and solar activity on the analyzed days were examined using the Kp, Dst and F10.7 cm indices.

Consequently, it was determined that the positive anomalies observed on days 286-292 may be related to moderate solar activity and/or the earthquake, and the positive anomalies observed on days 293, 294, 295, 296 (day of the earthquake) may be related to strong solar activity and/or the earthquake. Moderate solar activity and strong geomagnetic activity were observed for day 298, so the numbers of anomalies in both models increased dramatically. This increase is considered to be related to geomagnetic activity. The anomaly on day 298 may be related to the earthquake, geomagnetic effects and/or solar activity. The finding that the ionospheric conditions were variable in the analyzed days makes it highly difficult to identify earthquake-related ionospheric changes. Therefore, interdisciplinary study is needed to determine the earthquake-related part of the change in question.

REFERENCES

Arikan, F., Erol, C. B., Arikan, O.: Regularized Estimation of Vertical Total Electron Content from GPS Data for a Desired Time Period, Radio Science, 39:RS6012, 2004.

He, L. and Heki, K.: Ionospheric anomalies immediately before Mw 7.0-8.0 earthquakes. *Journal of Geophysical Research: Space Physics*, 2017.

He, L. Wu, L. Pulinets, S. Liu, S. Yang, F**.** A.: Nonlinear background removal method for seismo-ionospheric anomaly analysis under a complex solar activity scenario: A case study of the M9. 0 Tohoku earthquake. *Advances in Space Research*, *50*(2), 211-220, 2012.

Heki, K. and Enomoto, Y.: Mw dependence of the preseismic ionospheric electron enhancements. *Journal of Geophysical Research: Space Physics*, *120*(8), 7006-7020, 2015.

Kelley, M. C., Swartz, W. E., Heki, K.: Apparent ionospheric total electron content variations prior to major earthquakes due to electric fields created by tectonic stresses. *Journal of Geophysical Research: Space Physics*, 2017.

Kamogawa, M. and Kakinami, Y.: Is an ionospheric electron enhancement preceding the 2011 Tohoku-Oki earthquake a precursor?. *Journal of Geophysical Research: Space Physics*, *118*(4), 1751-1754, 2013.

Langley R. B.: Monitoring the Ionosphere and Neutral Atmosphere with GPS Division of Atmospheric and Space Physics Workshop, Frederiction, N.B., 2002.

Le, H., Liu, L., Liu, J. Y., Zhao, B., Chen, Y., & Wan, W. The ionospheric anomalies prior to the M9. 0 Tohoku-Oki earthquake. *Journal of Asian earth sciences*, *62*, 476-484, 2013.

Li, M. and Parrot, M.: Statistical analysis of the ionospheric ion density recorded by DEMETER in the epicenter areas of earthquakes as well as in their magnetically conjugate point areas. *Advances in Space Research*, 2017.

Liu, J. Y. Chen, C. H. Chen, Y. I. Yang, W. H. Oyama, K. I. Kuo, K. W.: A statistical study of ionospheric earthquake precursors monitored by using equatorial ionization anomaly of GPS TEC in Taiwan during 2001–2007. *Journal of Asian Earth Sciences*, *39*(1-2), 76-80, 2010.

Masci, F. Thomas, J. N. Villani, F. Secan, J. A. Rivera, N.: On the onset of ionospheric precursors 40 min before strong earthquakes. *Journal of Geophysical Research: Space Physics*, *120*(2), 1383-1393, 2015.

Namgaladze A. A. Zolotov O. V. Karpov M. I. and Romanovskaya Y. V. Manifestations of the Earthquake Preparations in the Ionosphere Total Electron Content Variations, *Natural Science,* Vol.4, No.11, 848-855, 2012

Nwankwo, V. U. and Chakrabarti, S. K. (2013). Effects of Plasma Drag on Low Earth Orbiting Satellites due to Heating of Earth's Atmosphere by Coronal Mass Ejections. *arXiv preprint arXiv:1305.0233*.

Pulinets S. A.: Strong earthquakes prediction possibility with the help of top side sounding from satellites. Advances in Space Research 21(3): 455−458, 1998.

Pulinets, S. and Davidenko, D.: Ionospheric precursors of earthquakes and global electric circuit. *Advances in Space Research*, *53*(5), 709-723, 2014.

Rozhnoi, A. Solovieva, M. Parrot, M. Hayakawa, M. Biagi, P. F., Schwingenschuh, K., Fedun, V.: VLF/LF signal studies of the ionospheric response to strong seismic activity in the Far Eastern region combining the DEMETER and ground-based observations. *Physics and Chemistry of the Earth, Parts A/B/C*, *85*, 141-149, 2015.

Schaer, S., Société helvétique des sciences naturelles. Commission géodésique. (1999). *Mapping and predicting the Earth's ionosphere using the Global Positioning System* (Vol. 59). Institut für Geodäsie und Photogrammetrie, Eidg. Technische Hochschule Zürich..

Şentürk, E., Livaoglu H., Çepni, M. S., A Comprehensive Analysis of Ionospheric Anomalies before Mw7.1 Van Earthquake on October 23, 2011, Journal of Navigation, DOI: 10.1017/S0373463318000826, 2018

Ulukavak, M. and Yalcinkaya, M.: Precursor analysis of ionospheric GPS-TEC variations before the 2010 M 7.2 Baja California earthquake. *Geomatics, Natural Hazards and Risk*, *8*(2), 295-308.

Thomas, J. N. Huard, J. Masci, F.: A statistical study of global ionospheric map total electron content changes prior to occurrences of M≥ 6.0 earthquakes during 2000–2014. *Journal of Geophysical Research: Space Physics*, *122*(2), 2151-2161, 2017.

Yao, Y., Chen, P., Wu, H., Zhang, S., Peng, W. Analysis of ionospheric anomalies before the 2011 M w 9.0 Japan earthquake. *Chinese Science Bulletin*, *57*(5), 500-510, 2012.

Yildirim, O. Inyurt, S. Mekik, C.: Review of variations in Mw< 7 earthquake motions on position and TEC (Mw= 6.5 Aegean Sea earthquake sample). *Natural Hazards and Earth System Sciences*, *16*(2), 543-557, 2016.

URL-1 https://omniweb.gsfc.nasa.gov/form/dx1.html